

## DIAELASTIC EFFECT IN ALUMINUM DUE TO LASER ULTRAVIOLET NANOSECOND LASER PULSE IRRADIATION

© 2025 G. V. Afonin<sup>a</sup>, V. Yu. Zhelezov<sup>b</sup>, T. V. Malinskiy<sup>b</sup>, S. I. Mikolutzkiy<sup>b</sup>, V. E. Rogalin<sup>b</sup>, Yu. V. Khomich<sup>b</sup>, N. P. Kobelev<sup>c</sup>, V. A. Khonik<sup>a,\*</sup>

<sup>a</sup>Voronezh State Pedagogical University (VSPU), Voronezh, Russia

<sup>b</sup>Institute for Electrophysics and Electric Power RAS (IEE RAS), Saint Petersburg, Russia

<sup>c</sup>Osipyan Institute of Solid State Physics RAS (ISSP RAS), Chernogolovka, Russia

\*e-mail: v.a.khonik@yandex.ru

Received July 03, 2024

Revised October 07, 2024

Accepted October 08, 2024

**Abstract.** It is shown that irradiation of single-crystal aluminum with nanosecond ultraviolet pulses, causing its surface melting, leads to a decrease in all resonance frequencies of the ultrasonic vibration spectrum of the sample. The shear modulus decreases from 0.87% to 1.45% with an increase in the incident radiation density from  $1.1 \text{ J/cm}^2$  to  $5.3 \text{ J/cm}^2$ . Subsequent heating to pre-melting temperatures causes the shear modulus to be restored to its original value. The hypothesis is argued that the discovered diaelastic effect is due to interstitial atoms in a dumbbell configuration, formed in the surface layer as a result of melting and preserved in this layer in a solid state due to the high rate of its cooling. The possibilities of another interpretation are discussed.

**Keywords:** *Nanosecond laser pulses, surface melting, ultrasound spectroscopy, shear modulus, interstitial atoms, dumbbell configuration*

**DOI:** 10.31857/S00444510250107e7

### 1. INTRODUCTION

Laser processing is one of the most promising and in-demand methods for modifying the physical properties of materials. The use of short laser pulses allows achieving high heating and cooling rates of the near-surface layer of the material [1]. It turns out that the behavior of solids during rapid processes changes significantly. This can lead to a fundamental alteration of properties, enabling the creation of materials with new mechanical, electrical, and optical characteristics. Pulsed lasers serve as a convenient tool for experimental research in the development of new materials and the study of their properties [2]. The results obtained using them provide broad opportunities for an in-depth understanding of such phenomena as phase transitions, recrystallization, formation of structural defects, amorphization, etc. [4, 3].

A particular interest lies in the use of laser pulses with a duration of about 10 ns and an energy density of several  $\text{J/cm}^2$ , leading to the melting of the surface layer of a substance within the duration of the pulse. The cooling of this layer occurs over a

time comparable to the pulse duration [5, 6], and the cooling rate when using nanosecond pulses can reach  $10^8 \text{ K/s}$  [7]. In the case of a pure metal, such a cooling rate is insufficient to form an amorphous layer (for example, pure vanadium and tantalum vitrify at a quenching rate of approximately  $10^{12} \text{ K/s}$  [8]; there is reason to believe that vitrification of monatomic metals is feasible in principle [9]). However, it is evident that its defect structure will undergo significant changes. Consequently, macroscopic elastic characteristics may also change, as the mechanical properties of crystals are largely determined by their defect structure. This experimental scheme was implemented in the present work. The object of study was chosen to be pure monocrystalline aluminum, subjected to nanosecond pulses of an ultraviolet laser, which induced melting of the surface layer and its subsequent rapid cooling (quenching).

The initial motivation for this work was as follows. Granato's well-known interstitialcy theory argues that metal melting results from the

avalanche-like generation of interstitial atoms in a dumbbell configuration (interstitial dumbbells), leading to a significant reduction in shear modulus and destabilization of the crystal lattice [10, 11]. The application of this theory to the case of multicomponent metallic glasses yields very good results, allowing a quantitative interpretation of changes in their properties during heat treatment in a solid amorphous state and tracing the connection between these changes and the properties of the melt and the parent crystal [11]. However, information on the applicability of these concepts to pure metals remains quite limited.

Firstly, it has been shown that monocrystalline aluminum in the premelting region exhibits a measurable diaelastic effect — a reduction in the shear modulus beyond the standard purely anharmonic decrease, indicating a significant increase in the concentration of interstitial dumbbells as the melting temperature is approached [12]. A similar situation is observed in polycrystalline indium [13]. Secondly, it was established that the observed premelting nonlinear increase in the heat capacity of aluminum can also be attributed to the intensive generation of interstitial dumbbells [14]. Finally, thirdly, about 70% of the total melting entropy of aluminum (and, accordingly, the heat of fusion) observed in experiments can be interpreted as the result of interstitial dumbbell generation at the melting temperature [15].

Based on this information, it was hypothesized that laser surface melting of aluminum would cause a significant increase in the concentration of interstitial dumbbell-type defects in the melt, and subsequent rapid cooling would “freeze” them in the solid crystalline state. The frozen interstitial dumbbells would induce a measurable diaelastic effect, the magnitude of which could indicate the concentration of these defects in the melt. However, other mechanisms of the diaelastic effect are also possible, as discussed below.

## 2. EXPERIMENTAL METHODOLOGY

Monocrystals of aluminum with a purity of 99.996%, grown using a modified Bridgman method with orientation 100 along the growth axis, were studied. Orientation control was performed using the X-ray method [12]. Samples in the shape of a cube with a side length of 3 mm were then prepared from the grown crystal using electrical discharge

machining. Each face of the cube was perpendicular to the [100] direction. The samples were then processed on a grinding machine with 1200-grit abrasive and annealed by heating to 923 K followed by slow cooling.

Sample processing was performed using a scanning laser beam from an Optolette HR2731 (OPOTEC Inc.), which generated radiation pulses with a wavelength of 355 nm, a duration of approximately 10 ns, an output energy of up to 2 mJ, and a pulse repetition rate of 100 Hz. The laser was calibrated using a Nova II energy meter (Ophir Optronics Solutions Ltd.) with a pyroelectric detector PE50-SH-V2. The laser spot size in the sample surface plane was determined using a standard method [16] by measuring the area of imprints left by laser pulses on a reference aluminum plate. The characteristic diameter of the laser spot in these experiments was 180  $\mu\text{m}$ . Surface processing of the sample was performed using a two-coordinate table, enabling sample movement along a “serpentine” trajectory at a speed of 3 mm/s with a line spacing of 25  $\mu\text{m}$ , ensuring that adjacent laser spots overlapped with a coverage coefficient of no less than 98%. Each area of the surface was exposed to 30 laser pulses. The energy densities on the surface of the processed samples exceeded the ablation threshold and were 1.1 J/cm<sup>2</sup>, 2.4 J/cm<sup>2</sup>, and 5.3 J/cm<sup>2</sup>. The exceeding of the ablation threshold was visually observed as an accompanying plasma plume and confirmed through electron microscopy images of the irradiated sample surfaces. All six faces of each cubic sample were sequentially processed. The surfaces of the samples before and after laser exposure were studied using a multi-beam optical profilometer Zygo NewView 7300.

The irradiated samples were then examined using resonant ultrasound spectroscopy (RUS) on a setup similar to that described in [17]. The excitation and detection of ultrasonic vibrations were carried out using piezoelectric transducers, which pressed the opposite vertices of the cubic sample. A special lever-type system minimized the axial pressure of the piezoelectric transducers on the sample, ensuring that the measured resonance spectrum was close to the natural one (i.e., determined only by the sample properties and its geometry). An advanced hardware-software RUS signal processing firmware enabled the registration of sample resonance frequencies with high precision, down to ppm levels. A total of

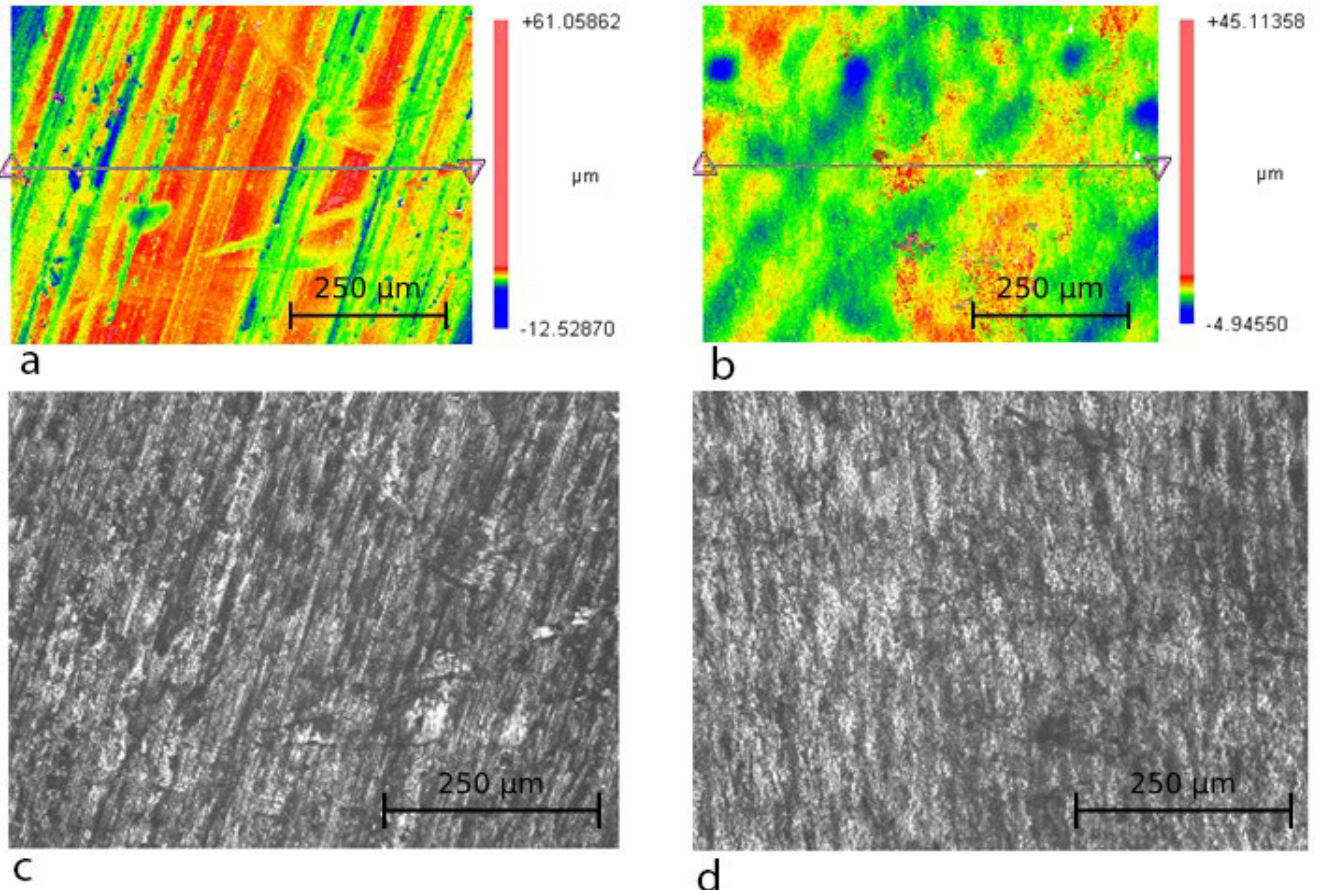


**Fig. 1.** (Color online) 2D profilograms (a, b) and surface micrographs (c, d) (optical profilometer Zygo NewView 7300) of sample S5 in the initial state (a, c) and after treatment with 30 UV laser pulses with an energy density of  $5.3 \text{ J/cm}^2$  (b, d).

five samples were studied in their initial state and after various laser treatments. The research results are illustrated below with data for three of them. Additionally, it should be noted that the time from sample irradiation to RUS measurement was several weeks.

### 3. RESULTS

Fig. 1 shows, as an example, 2D profilograms (a, b) and surface micrographs (c, d) of sample S5 in its initial state (a, c) and after laser exposure with 30 pulses at an energy density of  $W_p = 5.3 \text{ J/cm}^2$  (b, d). Linear morphological features in the initial state (a, c) correspond to abrasive processing traces. After laser exposure, these features disappear (b, d), and irregular roughness is observed on the surface, with a height comparable to that before irradiation. Detailed studies using a scanning electron microscope (SEM) revealed clear evidence of surface melting.

A similar situation was observed for treatments with other laser energy densities.

The RUS spectra of the studied samples over the full range of resonance frequencies ( $500 \text{ kHz} < f < 1300 \text{ kHz}$ ) contain 10–12 peaks corresponding to different elastic moduli and various interference modes due to the non-parallelism of the sample faces and other geometric defects. Fig. 2 shows the initial sections of the RUS spectra of samples S1, S3, and S5 after laser exposure at  $1.1 \text{ J/cm}^2$  (a),  $2.4 \text{ J/cm}^2$  (b), and  $5.3 \text{ J/cm}^2$  (c), followed by annealing via heating to  $850 \text{ K}$  and slow cooling, demonstrating the presence of several resonances. The differences in the absolute values of the resonance frequencies for different samples are due to variations in their geometric dimensions. It is evident that the resonance frequencies of the irradiated samples in all cases are slightly lower than those observed after annealing, while the resonance peak heights

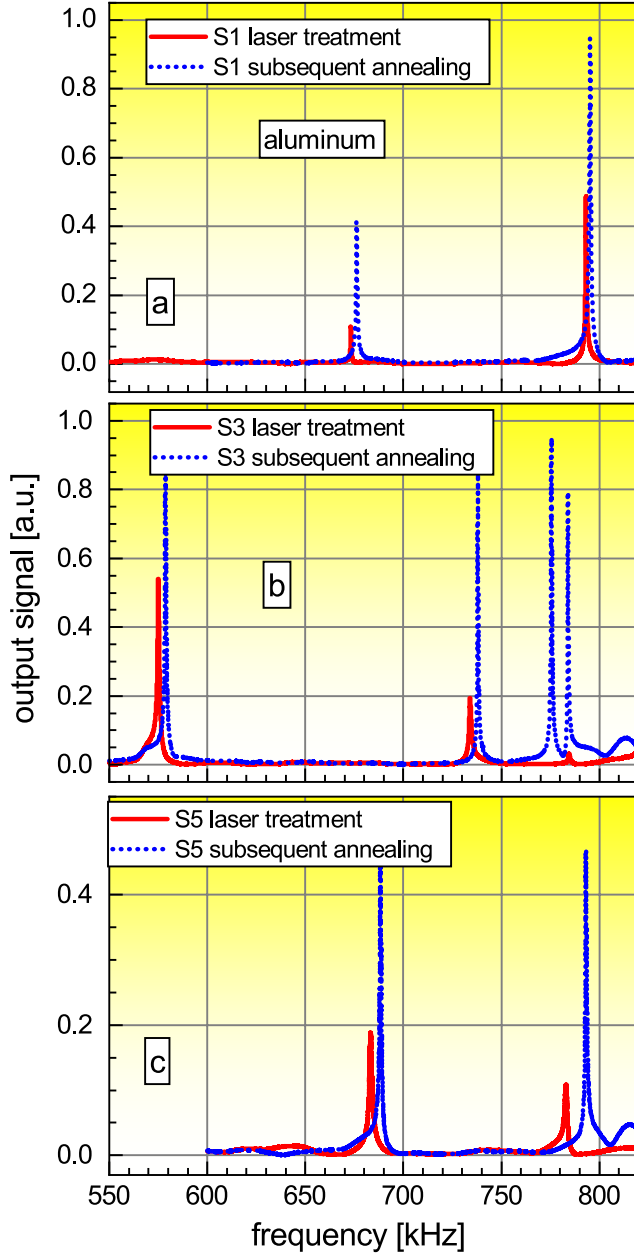


**Fig. 2.** (Color online) Initial sections of the resonant ultrasound spectroscopy spectra of aluminum samples S1 (a), S3 (b), and S5 (c), treated with UV laser pulses at energy densities of 1.1, 2.4, and 5.3 J/cm<sup>2</sup>, respectively. The spectra of the same samples after heating to 850 K at a rate of 3 K/min are also shown. It is evident that the resonance frequencies increase in all cases after annealing.

significantly increase after annealing, which unequivocally indicates a reduction in sample defectiveness. As is known, the lowest resonance frequency corresponds to pure shear vibrations and is controlled by the shear modulus ( $C_{44}$ ) [17]. This modulus (denoted as  $G$  hereafter) is of primary interest in this study.

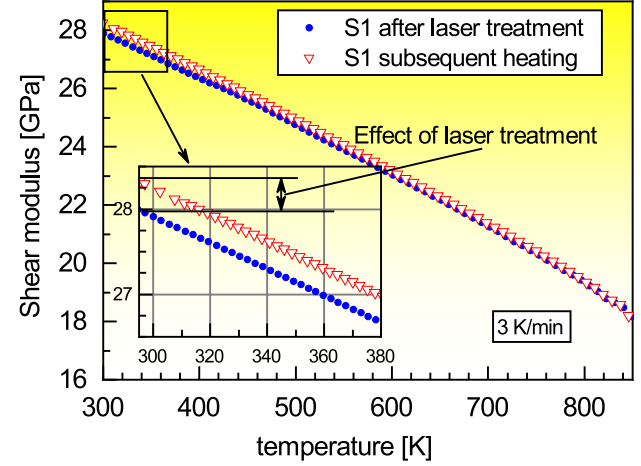


**Fig. 3.** (Color online) Temperature dependence of the shear modulus of sample S1 after laser exposure and subsequent reheating to 850 K. The inset shows the initial sections of these dependencies. Arrows indicate the effect of laser exposure on the shear modulus of the annealed sample. It is evident that heating to 850 K eliminates the influence of laser exposure on the shear modulus.

**Table.** Resonance frequencies of shear vibrations after laser exposure ( $f_{\text{irr}}$ ) and subsequent heating to 850 K ( $f_{\text{ann}}$ ), as well as the corresponding relative changes in the shear modulus ( $\Delta G/G$ ) for samples S1, S3, and S5, subjected to laser exposure at the specified energy densities ( $W_p$ ). The error in determining the resonance frequencies and their changes after annealing is approximately 5 ppm.

Sample No.	$W_p$ , J/cm <sup>-2</sup>	$f_{\text{irr}}$ , kHz	$f_{\text{ann}}$ , kHz	$\Delta G/G$
$S_1$	1.1	673.20	676.16	-0.0087
$S_3$	2.4	573.98	578.17	-0.0127
$S_5$	5.3	683.23	688.24	-0.0145

The table presents the resonance frequencies corresponding to the shear modulus for samples S1, S3, and S5 after laser exposure ( $f_{\text{irr}}$ ) and subsequent heating to 850 K ( $f_{\text{ann}}$ ) for three energy densities ( $W_p$ ). The relative changes in the shear modulus, calculated as

$$\Delta G/G = f_{\text{irr}}^2 / f_{\text{ann}}^2 - 1.$$

are also shown.

As seen, the shear modulus of sample S1 after irradiation at  $W_p = 1.1$  J/cm<sup>2</sup> is by 0.87% lower than after annealing. The decrease in the modulus after laser exposure increases with the energy of the incident radiation, reaching 1.45% for sample S5 at  $W_p = 5.3$  J/cm<sup>2</sup>. This is the diaelastic effect discussed in this work. Notably, this effect occurs not only for the shear modulus but also for all other elastic moduli, as all resonance frequencies in the RUS

spectrum decrease as a result of laser exposure (see Fig. 2). It is important to emphasize that no similar data are known in the literature.

#### 4. DISCUSSION

Metals, including the studied aluminum, absorb light through the transfer of photon energy to the electronic component of the skin layer, which has a thickness of approximately 10 nm [19]. The transfer of energy from the electronic subsystem to phonons takes several picoseconds. The heating time is approximately equal to the duration of the laser pulse and is of the order of 10 ns. At any of the applied laser energy densities  $W_p$ , surface melting of aluminum occurs, as confirmed by the aforementioned SEM observations of the irradiated sample surfaces. Simultaneously with the surface heating process, heat dissipation occurs due to thermodiffusion.

The characteristic heating depth during the laser pulse can be estimated as:

$$L = 2\sqrt{\alpha\tau}. \quad (1)$$

With  $\alpha = 9.7 \times 10^{-5} \text{ m}^2/\text{s}$  as the thermal diffusivity of aluminum and a laser pulse duration of 10 ns, using Equation (1), we obtain a heating depth of  $L \approx 2 \mu\text{m}$ . After the laser pulse ends, the cooling process of the heated region begins. The cooling time can be estimated from the equation [6]:

$$t_c = \frac{4L^2}{\alpha\pi^2} \ln\left(\frac{8T_m}{T_0\pi^2}\right), \quad (2)$$

where  $T = 933 \text{ K}$  is the melting temperature of aluminum, and  $T_0 = 300 \text{ K}$  is the initial temperature. Using Equation (2), the complete cooling time of the surface after laser exposure by a nanosecond pulse is  $t_c \approx 25 \text{ ns}$ . The cooling (quenching) rate from the liquid state can be estimated as  $T_v/t_c \approx 2 \cdot 10^{11} \text{ K/c}$ , where  $T_v = 2792 \text{ K}$  is the boiling temperature of aluminum. As noted earlier, this cooling rate is insufficient for amorphization of the pure metal. Thus, within about 25 ns, the surface layer undergoes a phase transition from the crystalline state to the liquid state and back.

Following the concept of melting of simple metals outlined in the introduction, we assume that melting of the surface layer results in a high concentration of interstitial dumbbell defects, which, due to subsequent rapid quenching, become “frozen” into the crystalline structure.

The key feature of an interstitial dumbbell is that an externally applied alternating mechanical stress induces oscillatory motion of 20–30 atoms near its core (the atomic structure of this defect is shown in [11, 20]), leading to significant inelastic deformation and a corresponding reduction in the shear modulus [11, 21].

For the shear modulus ( $G$ ) in the presence of interstitial dumbbells with a concentration  $c$ , the interstitialcy theory gives the relation [10, 21]:

$$G = G_0 \exp(-\alpha\beta_i c_i), \quad (3)$$

where  $G_0$  is the shear modulus of the defect-free crystal,  $\alpha \approx 1$  is a dimensionless constant, and  $\beta_i$  is the dimensionless shear susceptibility. Equation (3) shows that if the constant  $\beta_i$  is known, then by knowing the shear modulus of the defective crystal, one can estimate the concentration of interstitial dumbbells  $c_i$ , and vice versa.

A rough estimate using the Reuss approximation shows that the relative change in the shear compliance of the entire sample ( $\Delta S/S$ ) is related to the compliance change of the molten layer ( $\Delta S_{\text{irr}}/S_0$ ) by:

$$\Delta S/S = (\Delta S_{\text{irr}}/S)(\Delta V/V),$$

where  $\Delta V/V$  is the ratio of the molten layer volume to the sample volume. As noted earlier, the sample melts to a characteristic depth of  $L = 2 \mu\text{m}$ . The fraction of the molten part of the cubic sample with an edge length  $a$ , having six faces, is

$$\Delta V/V = 6L/a = 6 \cdot 2 \cdot 10^{-6} / (2.2 \cdot 10^{-3}) \approx 6 \cdot 10^{-3}.$$

Since for small changes in shear elasticity,  $\Delta S/S = -\Delta G/G$ , from table data, we find that  $\Delta S/S$  ranges from 0.009 to 0.014, depending on the laser energy density. Since shear compliance is the inverse of the shear modulus, the values of  $\Delta S_{\text{irr}}/S_0$  range from 1.5 to 2.3, corresponding to  $S_{\text{irr}}$  values ranging from 2.4S to 3.4S. Using Equation (3), for the shear compliance of the irradiated crystal, we take

$$S_{\text{irr}} = \exp(\alpha\beta_i c_i) / G_0,$$

where for interstitial dumbbells in aluminum  $\alpha\beta_i = 27$  [22]. Thus, the concentration of interstitial dumbbells  $c$ , which provides such compliance in the molten layer, should be 0.033 to 0.045.

Given the approximate nature of the initial data, this estimate appears reasonable. Indeed, calculations

of the interstitial dumbbell concentration for liquid aluminum using three independent methods give  $c_i \approx 0.08$  [15], which agrees with Granato's estimate for copper ( $c_i \approx 0.09$ ) [10]. On the other hand, computer simulations of aluminum melting have shown [23] that the shear modulus decreases from 14.9 GPa just below  $T_m$  to 1.8 GPa just above  $T_m$ . According to interstitial theory, the shear modulus of the melt is low but not zero. Using Equation (3), we estimate the interstitial dumbbell concentration at the melting temperature as:

$$c_i = \ln(14.9/1.8)/27 \approx 0.078,$$

which is close to the values obtained earlier. Finally, the pre-melting concentration of interstitial dumbbells in crystalline Al, based on precision shear modulus measurements, was found to be  $c_i \approx 0.004$  [12]. The obtained estimate  $c_i \approx 0.04$  after laser exposure is comparable to values at  $T_m$ , but, naturally, higher than pre-melting values.

Thus, these calculations are consistent with the understanding of the diaelastic effect in aluminum after laser exposure as a result of melting of the thin surface layer, accompanied by a sharp increase in the concentration of interstitial dumbbells, which remain largely frozen in the crystal due to high cooling rates. These frozen interstitial dumbbells define the observed diaelastic effect.

Other possible mechanisms for the shear modulus reduction after laser processing should also be considered. When exposed to a laser pulse, significant thermomechanical stresses arise in the sample. Assuming the temperature at the melt boundary is equal to the melting temperature of aluminum, while in the bulk of the sample, it remains close to room temperature, the temperature difference across the sample faces is approximately 600 K. Thus, the laser pulses generate high-amplitude mechanical pulses, which propagate through the entire sample. This corresponds to a relative total strain on the order of  $10^{-2}$ . This is a fairly large value, which can lead to plastic deformation of the sample due to dislocation formation. As is well known, an increase in dislocation density can lead to a reduction in the shear modulus [24]. To evaluate this mechanism, it is necessary to assess the dislocation density in the samples after laser processing.

Moreover, at high laser intensities, the formation of shock waves may occur as a result of the breakdown of the ablation plume [25]. In this

case, shock-wave-induced nanograin formation in the irradiated layer may take place, which could potentially contribute to the observed diaelastic effect.

A more detailed study of this phenomenon could provide new and important insights into the formation of the defect system in the crystal as a result of surface laser melting followed by high-speed cooling. It is also reasonable to expect that such experiments will lead to new significant information about the melting mechanism of simple metals.

## 5. CONCLUSION

For the first time, using resonant ultrasound spectroscopy (RUS), a diaelastic effect (reduction in elastic constants) has been detected in monocrystalline aluminum, induced by nanosecond ultraviolet laser pulses, which lead to melting of a thin near-surface layer of the sample. As a result of laser exposure, the shear modulus decreases from 0.87% to 1.45% with increasing incident energy density from 1.1 J/cm<sup>2</sup> to 5.3 J/cm<sup>2</sup>. Thermal treatment by heating to the pre-melting temperature range restores the shear modulus to its initial values, while a significant increase in the amplitude of RUS peaks indicates a substantial reduction in the material's defect density.

The hypothesis is put forward that surface melting is accompanied by the formation of a high concentration of interstitial defects in a dumbbell configuration, which are preserved in the solid state due to the high cooling rate of the molten layer. The inelastic deformation caused by these defects leads to the observed diaelastic effect.

Other possible interpretations of this phenomenon are also noted.

## ACKNOWLEDGMENTS

The authors express their gratitude to Professor D.L. Merson (Research Institute of Advanced Technologies, Tolyatti) for assistance in sample preparation, as well as to Professor I.A. Kaplunov, Associate Professor A.I. Ivanova (Tver State University), and Associate Professor V.V. Cheverikin (MISIS) for conducting electron microscopy studies.

## FUNDING

The RUS measurements and analysis of results based on interstitial theory were supported by the Russian Science Foundation, Grant No. 23-12-00162.

The laser irradiation, structural studies, and part of the discussion were carried out with the support of the Russian Science Foundation, Grant No. 24-19-00727, using the resources of the Tver State University's TsKp.

## REFERENCES

1. C. B. Anisimov, Ya. A. Imas, G. S. Romanov, and Yu. V. Hodyko. *Dejstvie izlucheniya bol'shoj moshchnosti na metally*, Nauka, Moscow (1970).
2. O. Zvelto. *Principy lazerov*, Lan', S-Pb, 2008.
3. V. Yu. Homich, V. A. Shmakov, Physics-Uspekhi **185**, 489 (2015).
4. V. E. Fortov. *Fizika vysokih plotnostej energii*, Fizmatlit, Moscow (2012).
5. S. I. Ashitkov, S. A. Romashevskii, P. S. Komarov, A. A. Burmistrov, V. V. Zhakhovskii, N. A. Inogamov, and M. B. Agranat, Quantum Electronics **45**, 547 (2015).
6. V. Yu. Zheleznov, T. V. Malinskiy, S. I. Mikolutskiy, V. E. Rogalin, S. A. Filin, Yu. V. Khomich, V. A. Yamshchikov, I. A. Kaplunov, and A. I. Ivanova, Pis'ma v ZhTF, **47**, 18 (2021).
7. M. von Allmen, S. S. Lau, M. Maenpaa, B.-Y. Tsaur, Appl. Phys. Lett. **36**, 205 (1980).
8. L. Zhong, J. Wang, H. Sheng, Z. Zhang, and S. X. Mao, Nature **512**, 177 (2014).
9. Tong, X., Zhang, YE., Shang, BS. et al. Nat. Mater. **23**, 1193 (2024)
10. A. V. Granato, Phys. Rev. Lett. **68**, 974 (1992).
11. N. P. Kobelev, V. A. Khonik, Physics-Uspekhi **193**, 717 (2023).
12. E. V. Safonova, Yu. P. Mitrofanov, R. A. Konchakov, A. Yu. Vinogradov, N. P. Kobelev, V. A. Khonik, J. Phys.: Condens. Matter. **28**, 1 (2016).
13. E. V. Goncharova, A. S. Makarov, R. A. Konchakov, N. P. Kobelev, V. A. Khonik, Pis'ma v ZhETF, **106**, 39 (2017).
14. E. V. Safonova, R. A. Konchakov, Yu. P. Mitrofanov, N. P. Kobelev, A. Yu. Vinogradov, V. A. Khonik, Pis'ma v ZhETF, **103**, 861 (2016).
15. R. A. Konchakov, A. S. Makarov, A. S. Aronin, N. P. Kobelev, V. A. Khonik, Pis'ma v ZhETF, **113** 341 (2021).
16. J. M. Liu, Optics Lett. **7**, 196 (1982).
17. F. F. Balakirev, S. M. Ennaceur, R. J. Migliori, B. Maiorov, and A. Migliori, Rev. Sci. Instrum. **90**, 121401 (2019).
18. G. Simmons and H. Wang, *Single Crystal Elastic Constants and Calculated Aggregate Properties*, Second edition, The MIT Press, Cambridge, MA (1971).
19. A. V. Sokolov. *Opticheskie svojstva metallov*, M.: Fizmatlit, 1961, 464 s.
20. R. A. Konchakov, A. S. Makarov, G. V. Afonin, M. A. Kretova, N. P. Kobelev and V. A. Khonik, Pis'ma v ZhETF **109**, 473 (2019).
21. A. V. Granato, Eur. J. Phys. B **87**, 18 (2014).
22. C. A. Gordon and A. V. Granato, Mater. Sci. Eng. A **370**, 83 (2004).
23. M. Forsblom and G. Grimvall, Nature Mater. **4**, 388 (2005).
24. A. S. Nowick, B. S. Berry, *Anelastic Relaxation in Crystalline Solids*, Academic Press, New York, London, (1972).
25. A. A. Ionin, S. I. Kudryashov, and L. V. Seleznev, Phys. Rev. E **82**, 016404 (2010).